Journal of Fluorescence, Vol. 5, No. 2, 1995

Fluorescence Lifetime-Based Biosensing of Zinc: Origin of the Broad Dynamic Range

Richard B. Thompson[1,2] and Marcia W. Patchan[1]

Fluorescence lifetime-based chemical sensors have recently been described for applications in medicine, environmental monitoring, and bioprocess control. These sensors transduce the level of the analyte as a change in the apparent fluorescence lifetime of an indicator phase. We have previously developed a wavelength-ratiometric fluorescence biosensor for zinc based on binding of zinc and dansylamide to apo-carbonic anhydrase which exhibited high sensitivity and selectivity. We demonstrate that the apo-carbonic anhydrase/dansylamide indicator system is very well suited for lifetime-based sensing, with a subnanomolar detection limit and greater than 1000-fold dynamic range. The theoretical basis for the wide dynamic range is discussed.

KEY WORDS: Biosensor; zinc sensor; lifetime-based sensing; carbonic anhydrase; dansylamide.

INTRODUCTION

Recently, optical sensing has emerged as an important new method for determining a broad range of chemical analytes in circumstances where classical chemical or instrumental analyses are difficult. Much of the work in the field of optical sensing has focused on fluorescence-based fiber-optic sensors, wherein the analyte of interest induces a change in the fluorescence of some indicator material or phase, which can be remotely measured through a length of optical fiber [1–4]. The pioneering fluorescence-based fiber-optic sensors relied on changes in the intensity of the fluorescence induced by the analyte and, consequently, were prone to artifact and hard to calibrate [4]. More recent sensors have relied on the analyte's inducing a wavelength shift in fluorescence, such that the analyte concentration is proportional to the ratio of fluorescence intensities at two wavelengths [5–7]. As Tsien and others have shown [8], this "wavelength-ratiometric" approach is much more robust and easier to calibrate. In particular, the ratiometric approach is practically immune to variations in excitation intensity, inner filter effects, scattering, and variations in the amount of the fluorescent indicator. Due to their robustness, wavelength-ratiometric approaches are very widely used for imaging ion concentrations within cells by means of fluorescence microscopy.

We adopted the wavelength-ratiometric approach in our development of a biosensor for zinc ion in solution; the basis for the sensor is depicted in Fig. 1. In our case the concentration was proportional to the ratio of fluorescence emission intensities at 450 and 550 nm. The goal of this sensor was to measure subnanomolar concentrations of zinc in solutions such as seawater which have potential interferents present at up to millionfold higher concentrations. We used an enzyme and fluorescent inhibitor as the indicator phase due to the very high selectivity of the enzyme active site for zinc over the likely interferents. In particular, we chose an enzyme, erythrocyte carbonic anydrase, which ordinarily binds zinc very tightly in its active site as a coenzyme; relatively few other metal ions can replace zinc [9–11]. It was discovered early on that many arylsulfonamides would inhibit the enzyme by replacing the hydroxide ion

[1] Department of Biological Chemistry, University of Maryland School of Medicine, 108 North Greene Street, Baltimore, Maryland 21201.
[2] To whom correspondence should be addressed.

1053-0509/95/0600-0123$07.50/0

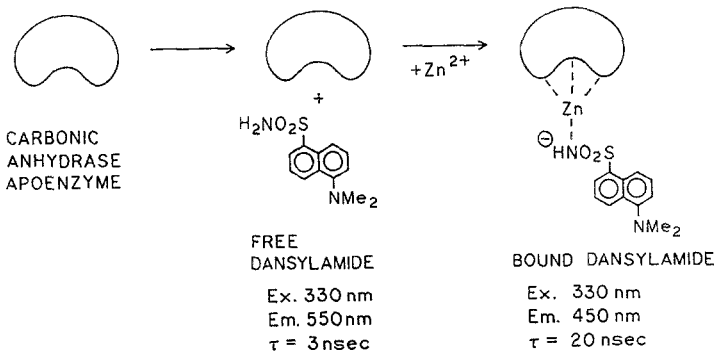

Fig. 1. Zinc sensing scheme employing carbonic anhydrase. In the absence of zinc the apoenzyme does not bind the fluorescent inhibitor dansylamide, and the typical weak, short lifetime, yellow–green emission of the dansylamide free in solution is observed. When zinc ion is added it is strongly bound by the enzyme, which permits the dansylamide to bind with concomitant strong, blue, long lifetime fluorescence.

ordinarily bound to the active site zinc; these inhibitors are of therapeutic value in treating glaucoma [10]. Chen and Kernohan [12] found that a fluorescent arylsulfonamide, dansylamide, would also bind to the active site as an inhibitor, and that the binding was accompanied by an increase in the quantum yield, a 100-nm blue shift, and a sevenfold increase in fluorescence lifetime of the dansylamide compared to its emission free in solution. We found that the dansylamide did not bind to the enzyme when the zinc had been removed, and therefore the binding of the inhibitor would report when the zinc was present (Fig. 1). Thus the presence of zinc (and therefore its concentration) would be transduced as the ratio of the fluorescence intensities from the free and bound dansylamide. While this approach was successful, it had a limited (20-dB) dynamic range and was difficult to employ with long lengths of optical fiber [7].

Particularly within the last year, sensors have emerged based on changes in the fluorescence lifetime of the indicator [13–21]. As discussed by Lakowicz [16,19], the lifetime-based sensing approach has nearly all the advantages of the wavelength-ratiometric approach and, in addition, is more flexible in terms of the indicators which may be used, since they can be based on different physical principles. Thus lifetime-based sensing has been demonstrated for glucose using a Förster energy transfer method [20], for oxygen based on collisional quenching [15,18], and for pH using indicators which exhibit different lifetimes in the acid and base forms [21]. Of course, to a first approximation fluorophores exhibit characteristic lifetimes, so calibration is facile. Work by Wolfbeis [15], Thompson *et al.* [22], Lakowicz [16], Berndt [23], and their colleagues suggests that lifetime-based sensing may be easier and less costly than believed only a few years ago.

An important attribute of lifetime-based sensing apparent (but little remarked upon [24]) in the work of Lakowicz and Szmacinski [21] is the very broad dynamic range available with lifetime-based sensing with suitable indicator phases. In the case of a simple mass action-driven equilibrium binding reaction (such as an antibody binding its antigen), the span of ligand concentration between when the ligand binding site is 10% occupied and when it is 90% occupied is almost 100-fold [25]. The dynamic range of sensors based on such reactions is then determined by the accuracy with which very small (or large) fractional binding site occupancies can be measured. For fluorescence intensity or intensity ratio measurements this is seldom better than a few percent, and consequently the dynamic range is typically about 100-fold. In contrast, Lakowicz and Szmacinski demonstrated a dynamic range of hydrogen ion concentration (pH) greater than 5.5 orders of magnitude (300,000-fold). Favorable circumstances for such a broad dynamic range would appear to include a substantial difference in lifetimes of the indicator (or indicator system) in the free and bound form, as well as a substantial wavelength shift in excitation and/or emission wavelength upon binding. Qualitatively speaking, the broad dynamic range is based on the fact that one can preferentially excite (or observe emission from) either the bound or the free form by judicious selection of the wavelength. Thus to see very small fractions of the acidic form of the pH indicator Carboxy SNARF-6, one must excite and observe emission from the dye at shorter wavelengths, where the basic form emits much more weakly. One goal of this paper is to establish the theoretical basis of this observation and, thereby, aid development of indicator systems with very broad dynamic ranges.

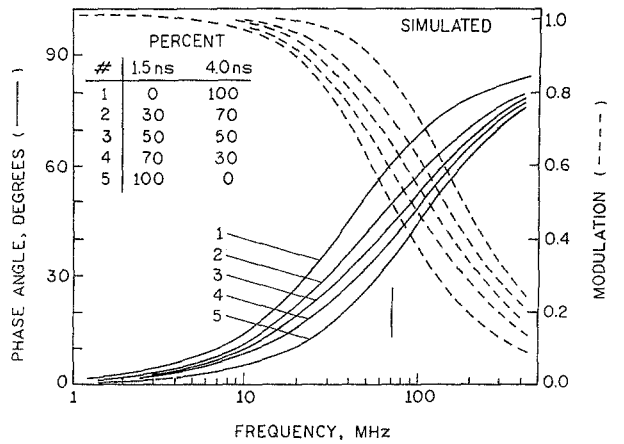

Fig. 2. Simulated frequency-dependent phase shifts and demodulations for a pH-sensitive fluorophore having a 1.5-ns lifetime in the acid form and 4.0 ns in the base form.

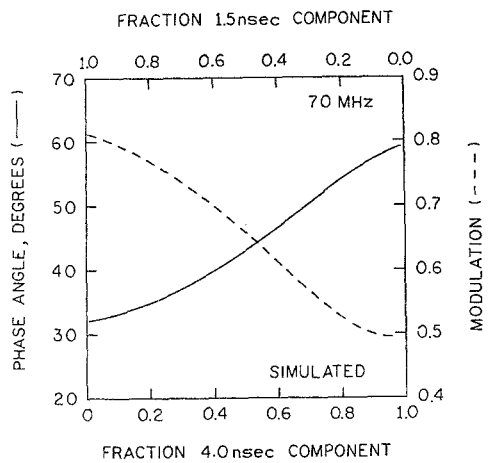

Fig. 3. Simulated phase shifts and demodulation at 60 MHz for a pH-sensitive fluorophore as a function of fraction of acid and base forms.

Inasmuch as the fluorescence lifetime of the bound dansylamide inhibitor increases approximately 7-fold, and the emission is blue shifted 100 nm, the carbonic anhydrase/dansylamide indicator system should permit measuring zinc concentrations over a greater than 1000-fold concentration range. Thus we decided to determine if lifetime based sensing was feasible with this system, and if so, what sort of dynamic range we could hope to achieve.

THEORY

The concept of lifetime-based sensing in the frequency domain is relatively straightforward [16,18,21,24]. Except in the case of a collisionally quenching analyte, one has some fluorescent indicator molecule whose lifetime differs substantially when the analyte is bound to the indicator compared to when it is not. In a frequency domain experiment, the frequency-dependent phase shifts and demodulations will vary, depending upon the fraction of the indicator present in each form [26]. An example of (simulated) data for such an indicator is shown in Fig. 2. In this case the indicator exhibits lifetimes of 4.0 and 1.5 ns in the free and bound forms, respectively. Note that while we hereafter consider the emission of each form to be a monoexponential decay for convenience, this need not be true to perform the analysis [27]. Data are shown for five fractions bound, from totally free to saturated. An advantage of lifetime-based sensing is that we can fit such frequency-dependent phase shifts and demodulations to double-exponential decay laws and recover the fraction present of the free and bound forms; if the concentrations are known, then the binding constant may be determined as well. This contrasts with other binding site titration methods, which typically require that at some point the binding site be saturated, which may be experimentally difficult or prohibitively costly. It is not necessary to acquire the entire frequency response as shown in Fig. 2. Suppose we plot the phase shifts at some suitable frequency (60 MHz in this example) as a function of fraction bound; the results of such a plot are depicted in Fig. 3. Such a curve is effectively a calibration curve, in that it is a single-valued function which depends only on the fractions present of the two forms, and their lifetimes. Experimentally this means that to quantitate the fraction bound (and thus the concentration), one need only pick some suitable modulation frequency and measure the phase (or modulation) at that frequency, suggesting that chemical sensing using this technique may be rather straightforward.

We wish to evaluate the potential for broad dynamic range of an indicator or indicator system which displays wavelength shifts in its fluorescence, as well as lifetime changes. We can specify the dynamic range as the concentration interval wherein the analyte concentration can be determined from the fraction bound, which in turn is determined from the measured phase shifts and demodulations at their typical level of precision and accuracy. Let us consider a case where free and bound forms are each described by monoexponential emission. Then the phase shift ϕ_ω and demodulation m_ω are given by

$$\phi_\omega = \arctan (N_\omega/D_\omega) \quad (1)$$

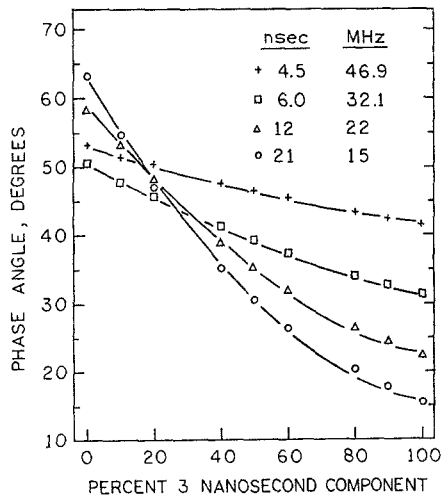

Fig. 4. Simulated phase shifts as a function of fractional intensity of the 3-ns component for two-component mixtures at selected frequencies. Thus the circles indicate the range of phase shifts at 15 MHz for a two-component mixture consisting of 3- and 21-ns lifetimes; triangles are for 3- and 12-ns lifetimes at 22 MHz; squares for 3- and 6-ns lifetimes at 32.1 MHz; and crosses for 4.5- and 3-ns lifetimes at 46.9 MHz.

$$m_\omega = \sqrt{N_\omega^2 + D_\omega^2} \tag{2}$$

where N_ω and D_ω are the sine and cosine transforms, respectively, of the time-dependent emission, and ω is the circular modulation frequency. Since the time-dependent emission may be described by a sum of exponentials,

$$I(t) = \sum_i \alpha_i e^{-t/\tau_i} \tag{3}$$

where α_i and τ_i are the preexponential factor and lifetime, respectively, of component i; N and D take the form

$$N_\omega = \sum_i \frac{\alpha_i \omega \tau_i^2}{1 + \omega^2 \tau_i^2} \Big/ \sum_i \alpha_i \tau_i \tag{4}$$

$$D_\omega = \sum_i \frac{\alpha_i \tau_i}{1 + \omega^2 \tau_i^2} \Big/ \sum_i \alpha_i \tau_i \tag{5}$$

The fractional intensity of each form f_i is related to the lifetimes and preexponential factors by

$$f_i = \frac{\alpha_i \tau_i}{\sum_i \alpha_i \tau_i} \tag{6}$$

If we assume that there are only two components present, then the ratio of the preexponential factors α is a simple function of the fractional intensities and the ratio of the lifetimes:

$$\frac{\alpha_2}{\alpha_1} = \frac{f_1 \tau_1}{f_2 \tau_2} \tag{7}$$

The fractional intensities are proportional to the product of the concentrations of the components C_i; the extinction coefficients $\varepsilon_{\lambda x}$ of the two components at the excitation wavelength λx; the quantum yields $Q_{\lambda m}$ of the two components at the emission wavelength λ_m; the excitation intensity $E_{\lambda x}$; optical factors O_x and O_m, representing the efficiencies of the excitation and emission optical trains, respectively; $D_{\lambda m}$, the detector responsivity, and some electronic gain factor G:

$$I_{tot} = \sum_i f_i \alpha \sum_i C_i \varepsilon_{\lambda x} E_{\lambda x} Q_{\lambda m} O_{\lambda x} O_{\lambda m} D_{\lambda m} G \tag{8}$$

Thus under the same set of instrumental conditions for both components, the fractional intensities will simply be a function of the absorbances, concentrations, and quantum yields of the two. In most of the cases examined to date the ratios of lifetimes and quantum yields do not exceed 10:1; this is unsurprising since low quantum yields and the consequent reduced intensities make it more difficult to collect precise lifetime data. If we further make the simplifying but inaccurate assumption that the quantum yield and absorbance of the indicator phase are about equal in the bound and free forms, we can predict the fraction bound (and thus concentration) dependence of the measured phase angles and modulations for various ratios of fluorescence lifetime of the free and bound forms. Such simulated data are plotted in Fig. 4. It is intuitively obvious and easy to see that the greater the ratio of lifetimes between the free and the bound forms of the indicator, the larger the difference in measured phase angle. Thus in Fig. 4 if the free form of the indicator has a 3-ns lifetime and the bound form has a 4.5-ns lifetime, at the suitable frequency of 46.9 MHz, the span of phase angles is only 11.5°, whereas if the bound form has a 21-ns lifetime (comparable to our zinc biosensor), the span is 47.4° at 15 MHz; analogous results are obtained for the modulation ratios (results not shown). The effects on precision and dynamic range of having a large phase angle difference are also apparent. At a fraction bound of 50%, with a 1.5:1 ratio of lifetimes the slope of the curve in Fig. 4 is 0.11° per %, whereas for a lifetime ratio of 7:1 it is 0.43° per % bound, almost fourfold steeper. If we have an accuracy and precision of phase measurement of 0.2°, the precision with which the fraction bound is known is ±2% bound in the former case and ±0.5% bound in

the latter. While the curves in Fig. 4 are not linear, the slope within each curve does not vary greater than two-fold, suggesting that the precision (and thus dynamic range) at the extremes of fraction bound will be at least comparable to that at 50% bound. At some point having a very large ratio of lifetimes (perhaps greater than 20: 1) would not usually enhance the phase angle span, since the phase angle difference cannot be greater than 90° at any frequency, and measuring large phase shifts (>75°) becomes less precise due to the nearly complete demodulation of the emission.

The curves in Fig. 4 are plotted assuming that the indicator in both the free and the bound forms has the same quantum yield at the emission wavelength and absorbance at the excitation wavelength. For the pH indicators studied by Lak and Szmacinski and the carbonic anhydrase/dansylamide/Zn system, this is manifestly not the case. In particular, by judicious choice of excitation or emission wavelength, one can effectively attenuate (reduce the apparent fractional intensity of) either the free or the bound form in comparison to the other. In the carbonic anhydrase/dansylamide/Zn example, we can preferentially observe a small amount of the bound form of dansylamide (such as would be seen at low Zn concentrations) in the presence of a large excess of the free form by simply shifting the wavelength at which the emission is observed to lower values. The changes in fractional intensities caused by shifting wavelengths [Eq. (8)] appear as apparent differences in the preexponential factors [Eqs. (6) and (7)] in the time-dependent emission [Eq. (3)], from whose sine and cosine transforms [Eqs. (4) and (5)] the phase and modulation may be calculated [Eqs. (1) and (2)]. More simply, if we know the excitation and emission spectra of the two forms, we can calculate a correction factor to apply to the apparent fractional intensity using Eq. (8). Thus for the carbonic/anhydrase/Zn system, we may choose an emission wavelength like 440 nm, where the normalized quantum yield of the bound form of dansylamide is about 1.0, and the normalized quantum yield of the free dansylamide is perhaps 0.02, or attenuated 50-fold. If by using a curve like that in Fig. 4, we determine a phase angle of 30.5°, corresponding to an apparent fractional intensity of 50% (1:1), the true ratio of free to bound is in fact 50:1 at 440-nm emission. Note that the phase angle is measured in comparison to the excitation or other reference, and not in comparison to the intensity at other wavelengths, which may be much greater. Also note that while we can effectively choose a concentration range within which to measure by selection of wavelengths, the accuracy and precision of the system at any wavelength band are set by the ratio of lifetimes of the free and bound forms.

EXPERIMENTAL

Human carbonic anhydrase II (recombinant) was a generous gift of Prof. Carol Fierke of Duke University; zinc was removed from the active site by treatment with 2,6-dipicolinic acid and affinity chromatography as described elsewhere [7,28,29]. 5,1-Dansylamide was from Aldrich and all experiments were performed in 50 m*M* HEPES, 150 m*M* Na_2SO_4, pH 7.3, as described previously [7]. Variable-frequency phase and modulation data were measured on an ISS K2 fluorometer (ISS, Champaign, IL) using dimethylPOPOP as a standard and fit to two-component decay laws as described previously [30,31]. The fluorometer has a Pockels cell modulator with a 250-MHz bandwidth; excitation at 325 nm is provided by a Liconix 4214NB HeCd laser with a 4.5-mW output (multimode). Emission bands were selected by the use of interference filters of 20-nm bandwidth centered at the indicated wavelength.

RESULTS AND DISCUSSION

We measured the frequency-dependent phase shifts and demodulations of the fluorescence emission of dansylamide both free and bound to native carbonic anhydrase over a range of concentrations and emission wavelengths. Measurements of the lifetimes of free dansylamide and dansylamide completely bound to native carbonic anhydrase gave largely monoexponential fitted values (20.6 and 3.0 ns) close to those measured by Chen and Kernohan using the slightly different excitation wavelength of the nitrogen lamp (22.1 and 2.6 ns) (results not shown) [12]. From mixtures of apoenzyme with excess dansylamide and varying concentrations of zinc added, we expect multiexponential decays which depend upon the zinc concentration and the emission wavelength. Concentrations were typically 9 μ*M* dansylamide and 3 μ*M* apoenzyme, chosen to assure that the dansylamide concentration was high enough (i.e., more than 10 times the K_d) to bind to any zinc in active sites and, also, somewhat in molar excess over enzyme in view of the lower quantum yield of the free dansylamide. Frequency responses measured at 480-nm emission wavelength for 3 μ*M* apoenzyme, 9 μ*M* dansylamide at several different zinc concentrations are shown in Fig. 5; similar data sets were obtained at emis-

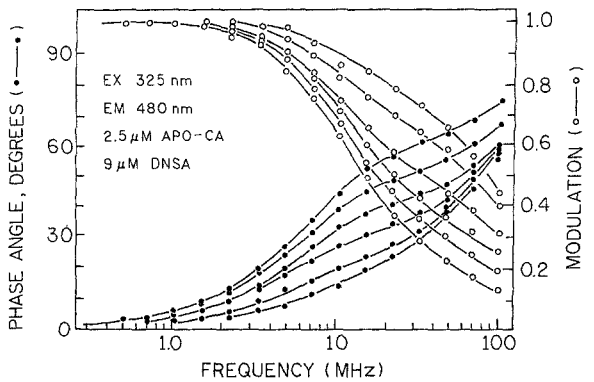

Fig. 5. Frequency-dependent phase shifts and demodulations for 9 μ*M* dansylamide and 3 μ*M* apocarbonic anhydrase measured at 480-nm emission for various concentrations of zinc. Reading phase angles upward at 10 MHz the concentrations are 0.5 n*M*, 10 n*M*, 30 n*M*, 100 n*M*, 300 n*M*, and 1 μ*M* zinc.

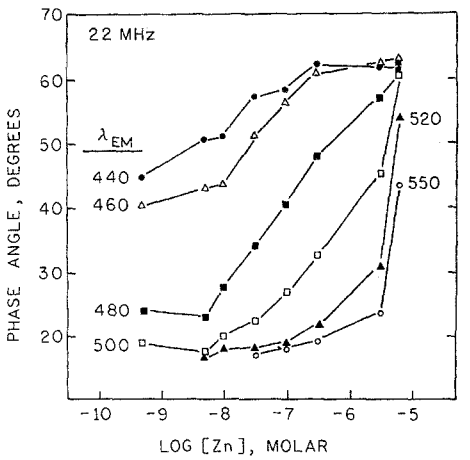

Fig. 7. Zinc concentration-dependent phase angles measured at various emission wavelengths.

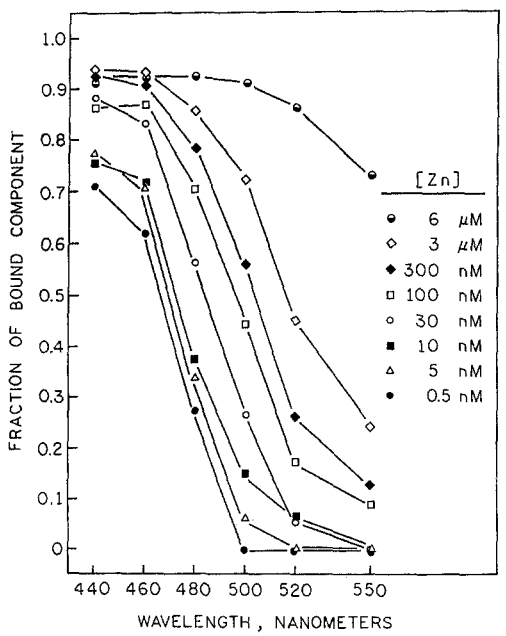

Fig. 6. Wavelength-dependent fractional intensities of the long-lifetime component derived from two-component fits to multifrequency phase data obtained for the indicated concentrations of zinc ion.

sion wavelengths of 440, 460, 500, 520, and 550 nm (results not shown). Four hundred eighty nanometers was chosen as a wavelength where emission from neither the free nor the bound forms of dansylamide dominates the emission. These data sets were fit to two component models, with the expected lifetime values usually being recovered to within 10%. Recovered fractional intensities from these fits (and those from frequency responses obtained at other wavelengths as well) are depicted in Fig. 6. As expected, the fractional intensity of the long lifetime component (bound dansylamide) at any wavelength increases with zinc concentration but decreases with wavelength at all zinc concentrations. The overlaps at short and long wavelengths simply reflect the difficulty of accurately recovering fractional intensities greater than 90 or less than 10%. The fact that the fractional intensity at 440 nm was still 70% at 0.5 n*M* Zn suggests that even lower concentrations could be measured using this technique; however, the intensity at this wavelength was quite low, leading to less precise data. We feel that this could be improved by the use of a more powerful excitation source: after modulation, less than 150 μW of UV power was available to excite the sample. These data also make apparent one of the virtues of this approach, namely, that the fractions of bound and free forms (and, knowing the K_d, the total ligand concentration) can be measured directly over a wide range of ligand concentration at a single concentration. Compare this with, for example, fluorescence polarization immunoassays which require that the entire range of polarization corresponding to completely free and fully bound be measured before the concentration can be known.

As discussed under Theory and depicted in Fig. 3, the phase shifts and demodulations for varying concentrations of analyte at some suitable frequency may be plotted to create a calibration curve; calibration curves consisting of phase angles at 22 MHz for the various emission wavelengths are depicted in Fig. 7. The corresponding modulation curves are roughly symmetric, as

seen earlier for pH indicators [21], and are not shown. For the concentration range between 1 n*M* and 1 μ*M* the best emission wavelength is 480 nm, since the phase angles range from roughly 20 to 53°. This concentration range is approximately the concentration range of interest for zinc in chemical oceanography and represents at least an order of magnitude improvement over the wavelength-ratiometric technique in the same system [7,32]. The data at shorter wavelengths for 0.5 n*M* Zn seem less precise, probably due to the relatively low signal levels. As suggested above, data at these lower concentrations might be improved and the detection limit extended by a brighter excitation source. In any case, our detection limit using lifetime-based measurements is significantly lower than that obtained with wavelength-ratiometric measurements (5 n*M*). The data at 520 and 550 nm are not less precise, but probably reflect the very low fraction of the emission contributed by the bound form. In general we expect these data to be akin to those of Lakowicz and Szmacinski, wherein the concentration-dependent phase angles appear as roughly sigmoidal curves offset in concentration for different wavelengths.

As described under Theory, it is feasible in principle to calculate the concentration of bound dansylamide (and thus zinc, since its binding is very tight) from the fractional intensity derived from a fit to a multifrequency data set, after correcting for the wavelength dependence of the excitation and emission. Similarly, for a two-component system (free and bound forms are monoexponentials) like this one, phase-sensitive fluorescence measurements [33] are capable of quantitating the free and bound forms. However, the procedure of constructing and using a calibration curve like those in Figs. 3 and 7 seems best, for three reasons. First, neither the free nor the bound forms need be a monoexponential. Second, measuring a phase and modulation at a single frequency can be done in microseconds [34], making it possible to follow the kinetics of binding reactions directly and obtain the results in real time. Since only a single frequency is required, for practical applications a phase fluorometer or sensor could be a much simpler, less expensive device. The phase angle vs concentration curves in Fig. 7 do not seem much noisier than the plots of fractional intensity versus wavelength in Fig. 6, even though the latter are fitted parameters derived from 30 or so data points and the former are single data points. One reason for this may be that much of the data collected at other frequencies for the fitted parameters contributes more to the noise than the signal. For instance, at conditions of low fraction bound the measured values of phase and modulation at high frequencies do not strongly influence the final result, but they contribute to the noise all the same. By comparison, one can pick one's frequency for maximum response, especially if a particular concentration range is known beforehand. Calibration curves like Fig. 7 are robust in that the lifetimes of the free and bound forms are properties of the molecules and thus unlikely to vary much. If temperature is maintained constant and oxygen levels in the sample are in equilibrium with the atmosphere, the calibration curve should be nearly invariant unless collisional quenchers are present or the pH is extreme. Note that even efficient collisional quenchers must be present at higher micromolar or low millimolar concentrations to perturb significantly the lifetimes of the fluorophores, unless they are very long.

Finally, there seems to be no reason in principle why ratiometric intensity measurements cannot also be performed over a wide concentration range. In particular, for many indicators one should be able to pick a wavelength where one form of an indicator is excited or emits predominantly, in order to see a small fraction of it in the presence of a much larger excess of the other form. Since the dynamic range of photomultiplier tubes (PMTs, the usual detector) is typically five orders of magnitude or more, it should be possible to measure intensities reproducibly over the same range and thus determine ratios of emission where the intensity of one measurement is much lower. Note that for lifetime measurements this is immaterial since the phase angle and demodulation of the perhaps weak emission are being compared to those of a standard compound or scatterer, whose intensity is arbitrary and can be matched with that of the sample. However, the effective dynamic range of PMTs at a single gain setting is not so great, perhaps three orders of magnitude. Thus to achieve a truly large dynamic range, a highly reproducible electronic gain control should be employed. An example of this is the solid-state fluorometer of Winefordner and colleagues, which uses an LED light source and PIN photodiode detector and is capable of intensity measurements linear over a large range [35].

CONCLUSIONS

We have demonstrated that zinc can be quantitated in solution over a broad concentration range and at low levels using fluorescence lifetime measurements and a suitable (biological) indicator. The data suggest that the detection limit may be extended with higher intensity excitation.

ACKNOWLEDGMENTS

The authors wish to thank Prof. Carol Fierke for the generous gift of recombinant carbonic anhydrase and the Office of Naval Research (H. Bright) and SERDP Program (W. Schulz and S. Snyder) for support. Some of these data were presented at the SPIE Conference on Chemical, Biochemical, and Environmental Fiber Optic Sensors held in Boston.

REFERENCES

1. R. B. Thompson (1991) in J. R. Lakowicz (Ed.), *Topics in Fluorescence Spectroscopy Vol. II: Principles*, Plenum Press, New York, pp. 345–365.
2. O. S. Wolfbeis (Ed.) (1991) *Fiber Optic Chemical Sensors and Biosensors, Vols. 1 and 2*, CRC Press, Boca Raton, FL.
3. D. Wise and L. Wingard (Eds.) (1991) *Biosensors with Fiber Optics*, Humana Press, Clifton, NJ.
4. S. M. Angel (1987) *Spectroscopy* **2**(4), 34–38.
5. C. Goyet, D. R. Walt, and P. G. Brewer (1992) *Deep-Sea Res.* **39,** 1015–1026.
6. S. Divers, S. D. Riccitelli, and M. Blais (1993) in F. P. Milanovich (Ed.), *Fiber Optic Sensors in Medical Diagnostics: SPIE Vol. 1886*, SPIE, Bellingham, WA, pp. 111–138.
7. R. B. Thompson and E. R. Jones (1993) *Anal. Chem.* **65,** 730–734.
8. R. Y. Tsien (1989) *Annu. Rev. Neurosci.* **12,** 227.
9. S. Lindskog *et al.* (1971) in P. Boyer (Ed.), *The Enzymes, Vol. 5*, Academic Press, New York, pp. 587–665.
10. S. J. Dodgson *et al.* (Eds.) (1991) *The Carbonic Anhydrases*, Plenum Press, New York.
11. J. E. Coleman (1965) *Biochemistry* **4,** 2644–2655.
12. R. F. Chen and J. C. Kernohan (1967) *J. Biol. Chem.* **242,** 5813–5823.
13. J. Wages, K. Hirshfield, and L. Brand (1987) *Biophys. J.* **51,** 284A.
14. S. M. Keating and T. G. Wensel (1991) *Biophys. J.* **59,** 186–202.
15. J. R. Bacon and J. N. Demas (1987) *Anal. Chem.* **59,** 2780–2785.
16. J. R. Lakowicz (1992) *Laser Focus* **28**(5), 60–80.
17. J. R. Lakowicz and R. B. Thompson (Eds.) (1993) *Advances in Fluorescence Sensing Technology I: SPIE Proc. Vol. 1885*, SPIE, Bellingham, WA.
18. M. E. Lippitsch, J. Pusterhofer, M. J. P. Leiner, and O. S. Wolfbeis (1988) *Anal. Chim. Acta* **205,** 1–6.
19. J. R. Lakowicz, H. Szmacinski, and R. B. Thompson (1993) in G. Cohn (Ed.), *Ultrasensitive Laboratory Diagnostics: Proc. SPIE Vol. 1895,* SPIE, Bellingham, WA, pp. 2–17.
20. J. R. Lakowicz and B. P. Maliwal (1993) *Anal. Chim. Acta* **271,** 155–164.
21. H. Szmacinski and J. R. Lakowicz (1993) *Anal. Chem.* **65,** 1668–1674.
22. R. B. Thompson, J. K. Frisoli, and J. R. Lakowicz (1993) *Anal. Chem.* **64,** 2075–2078.
23. K. Berndt (1987) *Measurement* **5**(4), 159–166.
24. R. B. Thompson and M. W. Patchan (1994) in R. Lieberman (Ed.), *Chemical, Biochemical, and Environmental Fiber Sensors V: Proc. SPIE Vol. 2068*, SPIE, Bellingham, WA, pp. 296–306.
25. G. Weber (1993) *Protein Interactions*, Chapman and Hall, London.
26. J. R. Lakowicz and I. Gryczynski (1991) in J. R. Lakowicz (Ed.), *Topics in Fluorescence Spectroscopy Vol. 1: Techniques*, Plenum Press, New York, pp. 293–335.
27. J. R. Lakowicz, H. Szmacinski, and M. L. Johnson (1992) *J. Fluoresc.* **2,** 47–52.
28. Y. Pocker and C. T. O. Fong (1983) *Biochemistry* **22,** 813–818.
29. P. L. Whitney (1974) *Anal. Biochem.* **57,** 467–476.
30. R. B. Thompson and E. Gratton (1988) *Anal. Chem.* **60,** 670–674.
31. E. Gratton, M. Limkeman, J. R. Lakowicz, B. P. Maliwal, H. Cherek, and G. Laczko (1984) *Biophys. J.* **46,** 479–486.
32. K. W. Bruland (1988) *Appl. Geochem.* **3,** 75.
33. J. R. Lakowicz and H. Cherek (1981) *J. Biol. Chem.* **256,** 6348–6353.
34. B. G. Pinsky, J. J. Ladasky, J. R. Lakowicz, K. Berndt, and R. A. Hoffman (1993) *Cytometry* **14,** 123–135.
35. B. W. Smith, B. T. Jones, and J. D. Winefordner (1988) *Appl. Spectrosc.* **42,** 1469–1472.